

Modeling the Constitutive Response of Metals Under Complex Loading

Alper UCAK¹

¹) Department of Civil Engineering, The Catholic University of America, Washington, DC

Abstract: In this paper, the different “built-in” material models based on the isotropic, kinematic and combined isotropic-kinematic hardening theories available in Abaqus/Standard are evaluated for carbon steels. Through a number of case studies the performance of the different “built-in” models are compared for different load paths. The similarities and differences between the available “built-in” material models are presented. Monotonic, quasi-static cyclic and dynamic load paths are considered. The results presented in this study are expected to provide important insight to practicing engineers dealing with inelastic material characteristics.

Keywords: Buckling, Constitutive Model, Impact, Low-Cycle Fatigue, Plasticity, Vibration.

1. Introduction

As the engineering community moves towards design concepts based on the performance of a component or structure, finite element methods gain popularity and become an indispensable tool. In finite element applications dealing with inelastic deformations, correct description of the material response is essential in order to arrive at an accurate and reliable prediction of the member or structural response. Inelastic characteristics of engineering materials are quantified with plasticity models based continuum mechanics. Different constitutive models aimed to describe the time-independent characteristics of engineering materials have been implemented to Abaqus (named as “built-in” models hereinafter). Applicable models for metals are the elastic-perfect plastic hardening model; linear, multi-linear or non-linear isotropic hardening model; linear or non-linear kinematic hardening model; combined isotropic-kinematic hardening model; and the Ramberg-Osgood model. All the above-mentioned material models are well known, and have successfully been used in a number of applications by practitioners and researchers. Furthermore it is possible to develop and integrate material specific constitutive models into Abaqus via user material subroutines (Ucak and Tsopelas 2008, 2011, 2012 among others).

From a practical point of view, the main difference between the above mentioned constitutive models might seem to be the number of material dependent parameters required for calibration, but in reality, these models differ from each other from a conceptual or mathematical point of view. Ideally, the constitutive model used in the finite element simulations should capture the base material response (or the macroscopic response) under monotonic, and proportional and non-proportional random cyclic load paths. However, more often than not, such a model might not be readily available. If this is the case, the burden is on the analyst to pick and choose the correct “built-in” constitutive model.

In this paper, the different “built-in” material models for metals available in Abaqus/Standard are evaluated for carbon steels. Through a number of case studies the performance of the different “built-in” models is compared for different load paths. Specifically we concentrate on the following questions: (a) the importance of capturing the cyclic stress-strain curve and possible pitfalls in material model/calibration; (b) and the importance of capturing the shape of the hysteresis curves. Temperature and strain rate effects are not considered in this study. Although we focus only on carbon steels, the observations reported herein might also be applicable to other metals such as stainless steel. The results presented in this study are expected to provide important insight to practicing engineers dealing with inelastic material characteristics.

2. Macroscopic Response of Carbon Steels

The macroscopic characteristics of metals are quantified with monotonic and cyclic coupon tests. Figure 1 depicts the composite monotonic and cyclic stress-strain curves for a mild structural steel with a sharp yield point (ASTM A36), and a low-yield point steel with smooth elasto-plastic transition (LYP 100). The cyclic trends presented in Figure 1 are obtained by connecting the locus tips of stable hysteresis curves from tests conducted at room temperature, very low strain rates, and different strain amplitudes, at which the strain is completely reversed.

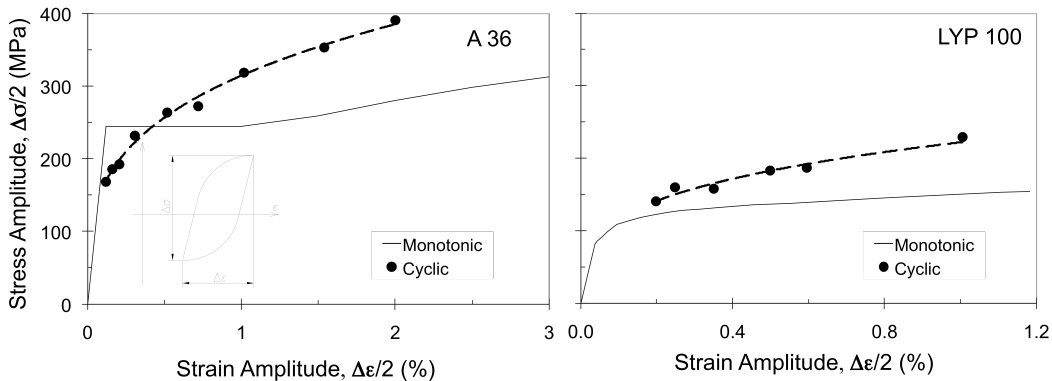


Figure 1. Monotonic and cyclic stress-strain curves of A36 and LYP 100 grade steels.

As shown in Figure 1, during monotonic loading, after the elastic deformation the A36 grade steel shows a sharp yield point followed by a yield plateau. The plastic deformation along the yield plateau is caused by Luders band propagation. Once the Luders bands cover the whole gage, the material starts hardening. On the other hand, the LYP 100 grade steel shows a highly non-linear (and smooth) elastic-plastic transition followed by hardening.

For metals, the monotonic loading curve may not be representative of the cyclic response characteristics of the material. The experimental data presented in Figure 1 indicates that this statement is correct for both A 36 and LYP 100 grade steels. The observed response under reversed loading is either amplitude-dependent cyclic hardening or softening. The A 36 grade steel undergoes cyclic softening for cyclic strain amplitudes smaller than $\Delta\epsilon/2 \sim 0.5\%$, and cyclic

hardening for amplitudes larger than this threshold. The LYP 100 grade steel does not undergo cyclic softening, and the observed material response under reversed loading is cyclic hardening. The data presented in Figure 1 indicates that the cyclic characteristics of carbon steels cannot be quantified using the monotonic hardening curve.

3. Brief Description of the Material Models Available in Abaqus/Standard

Constitutive models are used to describe macroscopic properties of engineering materials. Different constitutive models aimed to describe the time-independent material response of metals have been implemented to Abaqus/Standard, namely, constitutive models based on isotropic hardening, kinematic hardening and combined isotropic-kinematic hardening. All these models are based on a von Mises yield criterion, and an associative flow rule, which are common assumptions made in describing the constitutive behavior of metals. On the other hand, none of the above mentioned models consider a memory surface (in the strain space).

In the isotropic hardening theory, it is assumed that the yield surface expands uniformly in the stress space as a function of a selected internal variable, generally the accumulated plastic strain. In the kinematic hardening theory, the yield surface is assumed to translate in the stress space along the direction of the plastic strain increment. While from a theoretical point of view, the idea behind isotropic and kinematic hardening theories are totally different, for practical considerations, their similarities/differences are summarized below for different loading protocols consisting of; (a) monotonic loading; (b) constant or increasing amplitude cyclic loading; (c) variable amplitude cyclic loading.

4. The Importance of Correct Description of the Material Response

4.1 Monotonic Loading

The monotonic stress-strain curves of carbon steels with a sharp yield point or a smooth elasto-plastic transition can be accurately simulated with the “built-in” material models available in Abaqus/Standard. Figure 2 depicts the comparison of the simulated monotonic stress-strain response of LYP 100 steel with the experimental one. Two different simulations are conducted. In the first one a combined non-linear isotropic and kinematic hardening model is utilized, whereas in the second one a multi-linear isotropic hardening model is used. As evident from Figure 2, the agreement between the experimental data and the simulations are excellent. It is also noted that the monotonic stress-strain curve produced by the two different models are virtually identical. It is very important to note that the monotonic response of LYP 100 could also be simulated with the Ramberg-Osgood model, or the non-linear kinematic hardening model with two back-stress components (with the recall term of the second component being close to zero) with the same accuracy.

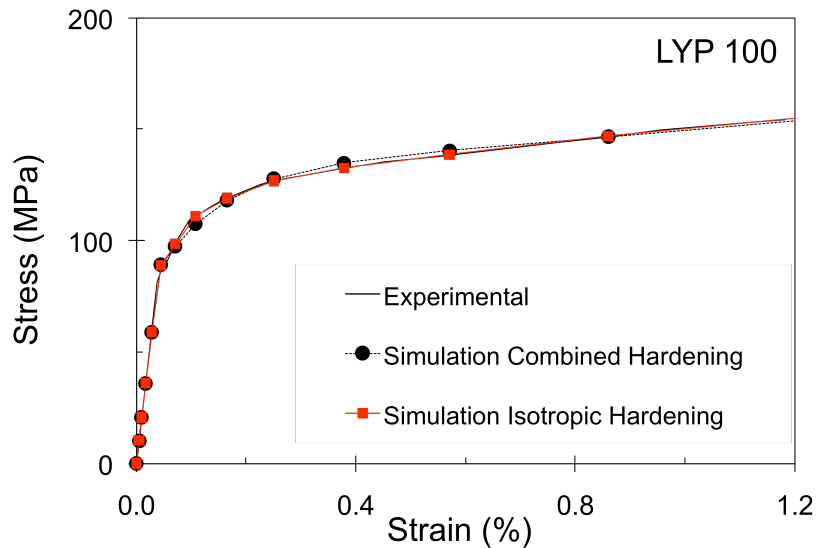


Figure 2. Simulated monotonic response of LYP 100 steel.

While the multi-linear isotropic hardening, and the combined non-linear isotropic and kinematic hardening models produce the same monotonic stress-strain response, the hysteresis curves produced by these two models under cyclic loading will be totally different. Figure 3 depicts the simulated cyclic response of LYP 100 steel for a cyclic loading amplitude of $\Delta\varepsilon/2=0.5\%$. The multi-linear isotropic hardening model, for which the expansion of the yield surface (or the hardening) is based on accumulated plastic strain, shows cyclic hardening without saturation. In the combined hardening model, the non-linear isotropic hardening component is calibrated to simulate the smooth elasto-plastic transition, and the kinematic part is calibrated to simulate the hardening part (see Figure 2). In other words, the non-linear isotropic hardening component in the combined model will saturate once the elasto-plastic transition is completed. Hence, as shown in Figure 3, the combined model shows almost no cyclic hardening. If, for example a finite element analysis is conducted to study buckling of a stock plate made of LYP 100 steel, while the buckling load obtained for monotonic loading using the isotropic and combined models would be similar, it is evident from Figure 3 that the buckling load of the same plate predicted under cyclic loading will be different for the isotropic and combined models.

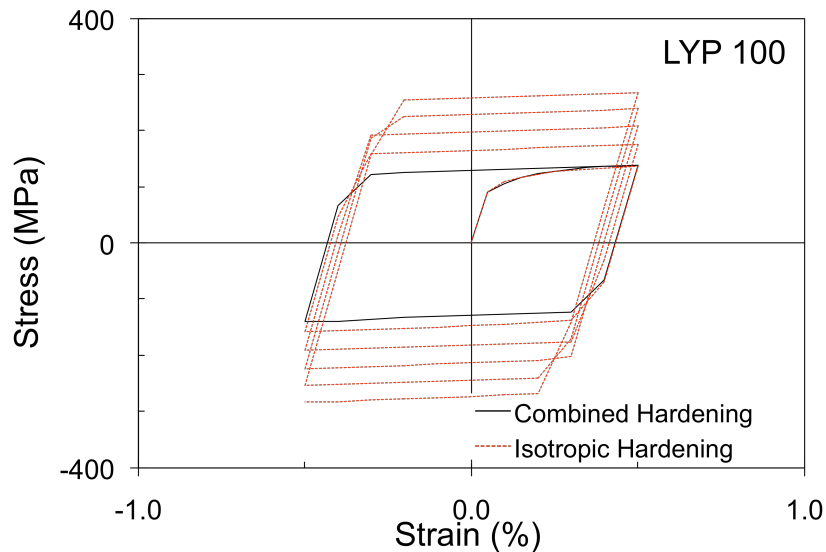


Figure 3. Simulated cyclic response of LYP 100 steel with the multi-linear isotropic and combined isotropic-kinematic hardening models.

4.2 Constant or Increasing Amplitude Cyclic Loading

For load paths consisting of constant or increasing amplitude cyclic loading, it is possible to use the non-linear kinematic hardening model, the non-linear isotropic hardening model, or the combined non-linear kinematic-isotropic hardening model and get satisfactory results. However, it is very important to note that the above-mentioned material models are used to describe macroscopic properties of the base material. Hence, the material dependent parameters that are required by the particular constitutive model shall be calibrated solely using experimentally determined monotonic and cyclic coupon data, and they should not be ‘fine-tuned’, so that the finite element results agree better with the experimental ones.

For example, assume a parametric finite element study, were the factors affecting the strength and ductility of stocky plated steel components (like steel columns, steel beams, steel shear walls etc.) are investigated under quasi-static cyclic loading. Here with stocky, we mean components that will undergo elasto-plastic buckling, such that the base material will experience stresses and strains well above the yield stress and strain.

Usually, for these studies two sets of experimental data will be available to the analyst; (1) monotonic and cyclic coupon data of the base material the component is made of, which will be used to calibrate the constitutive model; (2) a limited number of cyclic experimental data of the component, which will be used to verify the global accuracy of the finite element model.

After the material model is calibrated using the experimental coupon data, and the results of the finite element model is verified with the experimental ones, usually a parametric study is conducted, for example, to study the effect of plate thickness, stiffener spacing etc. However, care

should be taken if ‘built-in’ constitutive models based on isotropic and/or kinematic hardening models are utilized in the study.

4.2.1 Calibration/Validation of the Material Model: Possible Pitfalls

Herein, we study the elasto-plastic buckling of three stocky square steel columns under constant axial and cyclic lateral load (Figure 4). All three columns were tested by Nakamura et al. (1997). The base material used to build-up the columns was mild structural steel with a yield plateau, JIS grade SM 490 (ASTM A242 equivalent). All three columns were made of the same base material with an initial yield stress equal to 374 MPa (± 3 MPa), and the only differences between them were the plate thicknesses and stiffener spacing. Since all three columns were made of the same base material, the global response of all three columns should theoretically be captured with the same material model and the same set of material dependent parameters.

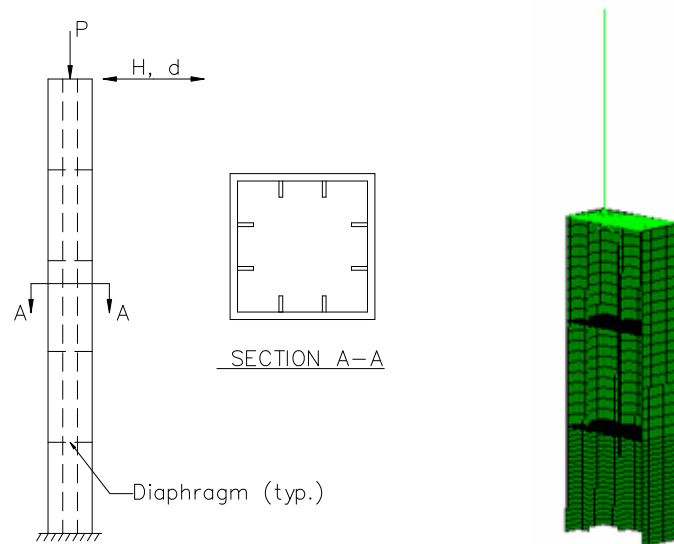


Figure 4. Schematic presentation of the experimental setup and corresponding finite element model.

The finite element model used is depicted in Figure 4. It consists of SR4 shell elements, B33 beam elements and RB2D2 rigid links, all of which are available in Abaqus/Standard element library. Using symmetric boundary conditions only half of the column is discretized in the analyses. At the base, fixed boundary conditions are applied. Preliminary analyses conducted have shown that in box section stiffened cantilever steel columns, localized deformation is concentrated in the lowest section of the column, close to its base, which is in agreement with the experimentally established deformation patterns. Given this typical behavior only the lower half of the column is discretized with SR4 shell elements (including flange, web, vertical stiffeners and diaphragms) while the upper part is modeled using B33 beam elements. The beam elements are connected to shell elements using rigid links.

In the simulations, the macroscopic response of the base material is simulated with the nonlinear kinematic hardening model. Two sets of analyses are conducted, called “NLKH-Set 1” and “NLKH-Set 2”. In “NLKH-Set 1” the cyclic characteristics of the base material are ignored and the material dependent model parameters are calibrated using the monotonic stress-strain curve of the material. In “NLKH-Set 2”, the material dependent parameters are calibrated using the hardening part of the cyclic hardening curve. The resulting stabilized stress amplitudes along with the experimental monotonic and cyclic trends are presented in Figure 5.

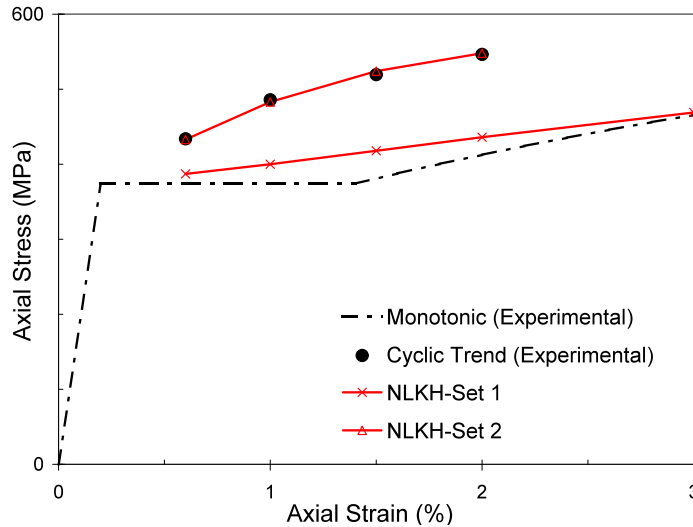


Figure 5. Idealized material response.

Figure 6 compares the hysteretic loops obtained from the FEM analyses with “NLKH-Set 1” parameters with the experimental ones reported by (Nakamura et al. 1997). In Figure 5, the normalized horizontal displacement at the loading point is plotted in the abscissa and the corresponding normalized shear force (horizontal force) is plotted in the ordinate. An inspection of the hysteretic curves presented in Figure 6 shows that for column KD1, the numerical results obtained with the “NLKH-Set 1” are in excellent agreement with the experimental results. The FE model predicts shape of the hysteresis curves, the buckling load, the maximum deformation capacity, as well as the stiffness deterioration and the strength degradation accurately. However, the same figure also indicates that the FE models with the “NLKH-Set 1” material parameters perform poorly for columns KD 2 and KD 3. For both columns the buckling load and the maximum deformation capacity and the shape of the hysteresis curves are not predicted correctly. This is due to the fact that columns KD 2 and KD 3 are stockier compared to KD 1, and can take advantage of the cyclic hardening characteristics of the base material, prior to buckling.

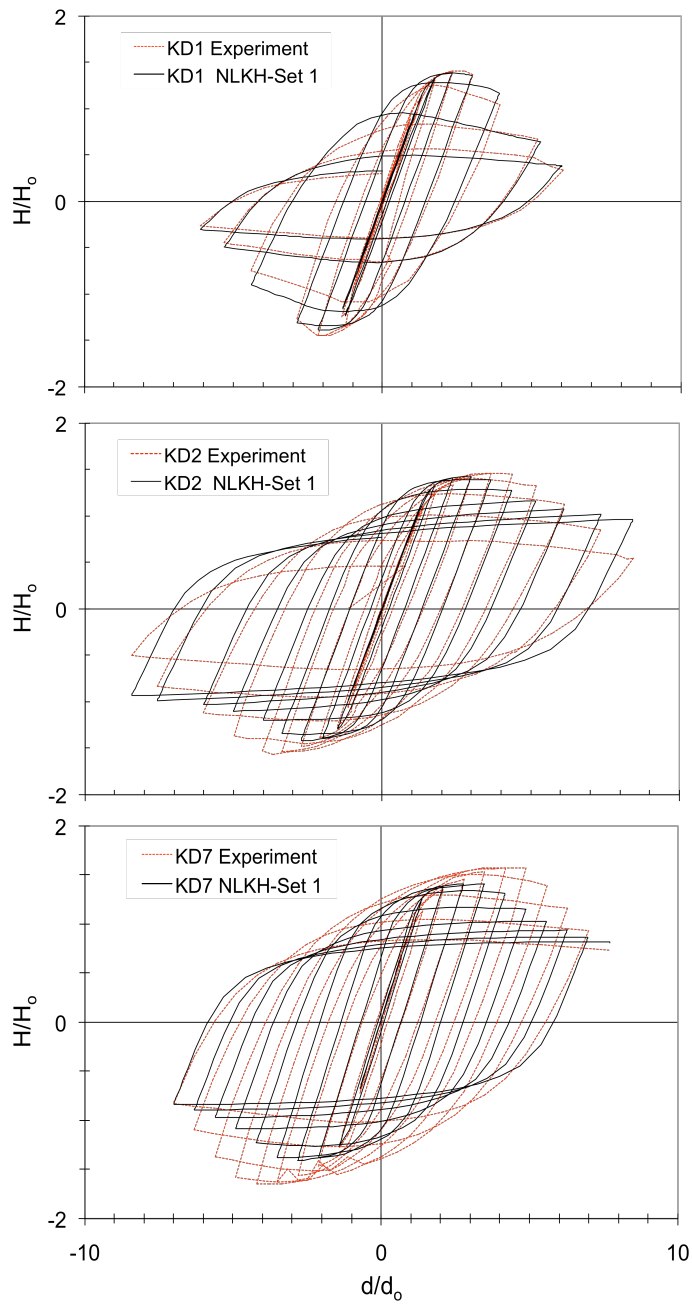


Figure 6. Experimental versus FEM analyses results with Set 1 parameters.

Figure 7 compares the hysteretic loops obtained from the FEM analyses with “NLKH-Set 2” parameters with the experimental ones. An inspection of the hysteretic curves presented in Figure 6 shows that for column KD 7, the numerical results obtained with the “NLKH-Set 2” are in satisfactory agreement with the experimental results. The FE model predicts shape of the hysteresis curves, the maximum deformation capacity, however slightly over-estimates the positive maximum lateral load capacity. However, the same figure also indicates that the FE models with the “NLKH-Set 2” material parameters dangerously over-estimate the lateral force capacity of columns KD 1 and KD 3.

For this parametric study, the experimental hysteresis curves for the three columns tested by Nakamura et al. (1997) were available to the authors, and the performance of different material models could easily be determined. However, the results presented in Figure 6 and 7 show that, validating the accuracy of the material model (and the material dependent parameters) using one benchmark specimen with a particular slenderness does not guarantee that the material model or the selected material dependent parameters can be used with the same accuracy to capture the response characteristics of a specimen with different slenderness.

4.3 Dynamic Loading: The Importance of Capturing The Shape of the Hysteresis Curves

In the quasi-static cyclic buckling analyses presented in Section 4.2, the material models were calibrated using the cyclic stress-strain curve of the base material. In other words, the objective was simulating the stabilized stress amplitudes (for given strain amplitudes), and not the shape of the stress-strain loops. To investigate the importance of simulating the shape of the base material stress-strain loops under cyclic loading correctly, dynamic analyses are conducted next.

Trimble and Krech (1997) documented a series of experiments, in which cantilever beams made of HY-80 grade steel were subjected to transient dynamic loads. The test program was designed to study the nonlinear dynamic response of simple structures, and consequently to investigate the ability of elastic-plastic analysis techniques to predict the dynamic response of components made of HY-80 steel. One of the tested specimens in the above-cited study (referred to as CL-3) was used as benchmark verification example to investigate the performance of the various constitutive models.

The schematic presentation of the experimental setup documented by Trimble and Krech (1997) is shown in Figure 8. The vertical cantilever test consists of 14 x 4 x 0.375 inch thick HY-80 specimen plate with a steel mass block at the cantilever tip. This assembly is welded to a thick support plate and bolted to a parallel pendulum shock machine. The parallel pendulum machine is essentially a table that is suspended vertically by steel cables. The table is raised to the test position and allowed to swing pendulum-style into a stop wall. The impact applies a lateral impulse load to the test article, which excites the mass block and induces a bending response in the specimen. The machine is capable of obtaining different load severity levels and pulse durations. During the experiments the acceleration and the deformation of the cantilever tip and the surface strains at different locations were measured.

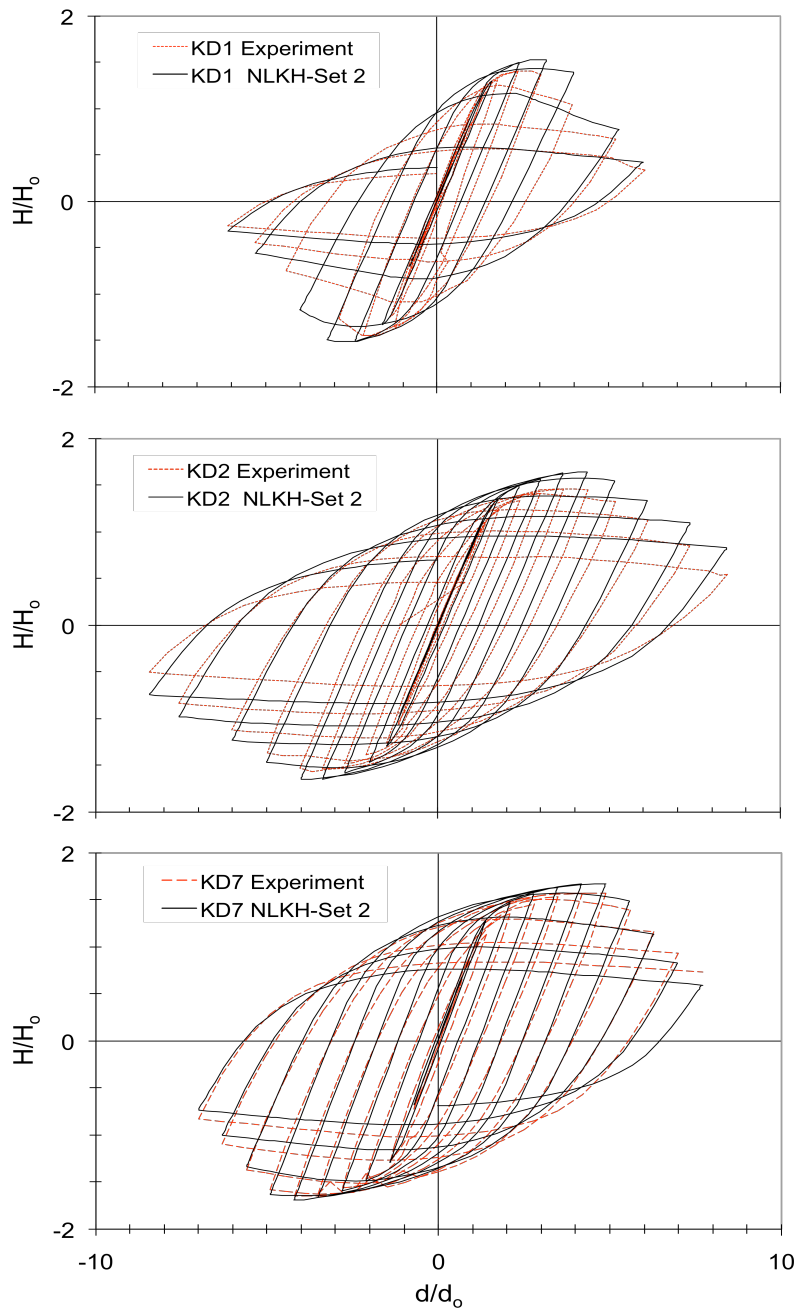


Figure 7. Experimental versus FEM analyses results with Set 2 parameters.

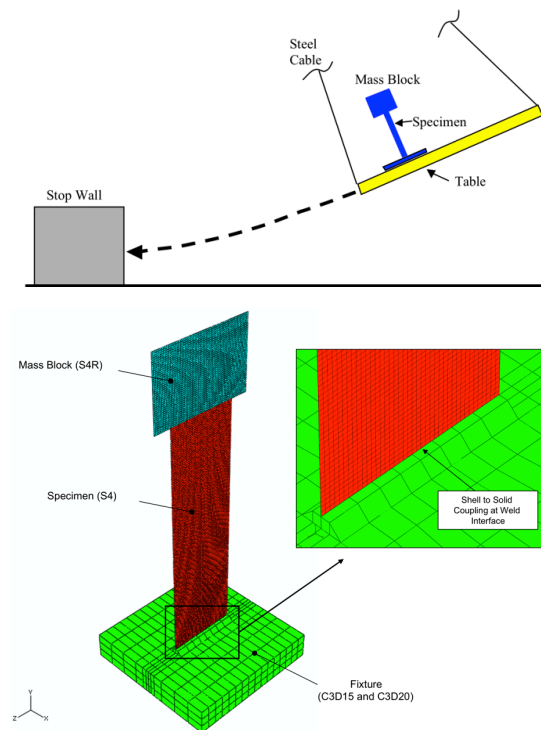


Figure 8. Schematic presentation of the experimental setup used by Trimble and Krech (1997) and the corresponding finite element model.

The finite element model used for the vertical cantilever beam assemblies is also shown in Figure 8. The model includes explicit representations of the specimen, mass block, mounting fixture, and the weld between the specimen and the fixture. The model is constructed using the nominal construction dimensions of the specimens. The specimen plate is the main region of interest and it is represented by 0.375" thick fully integrated shell elements (S4) with a mesh density of approximately 0.1"x0.1". The mass block included in the model undergoes rigid body motion, and only represents the cantilevered weight. As such, the mass block is represented with 5" thick reduced integration shells (S4R), mainly for computational efficiency. The mounting plate and weld are explicitly represented by 2nd order continuum elements (C3D20, C3D15). As shown in Figure 8, the interface between the specimen and the weld is modeled using surface-based distributing couplings, which were created using the shell-to-solid coupling. In the finite element analysis the initial imperfections and the initial residual stresses, which may have been caused by welding are ignored, and the specimens are excited at the cantilever base with the actual transient accelerations.

Two sets of simulations are conducted. In the first set the material response is modeled with the multi-linear isotropic hardening model. In the second set the kinematic hardening model is used to describe the constitutive response of the base material. The material dependent properties used are calibrated using the experimental data reported by Hodge et al. (2003). Figure 9 depicts the

comparison between the simulated monotonic stress-strain curves with the experimental one. An inspection of Figure 9 shows that the multi-linear isotropic hardening model can accurately simulate the monotonic response of HY 80 grade steel, including the plateau response. The linear kinematic hardening model cannot capture the initial plateau response, but the overall agreement with the experimental data is reasonably well.

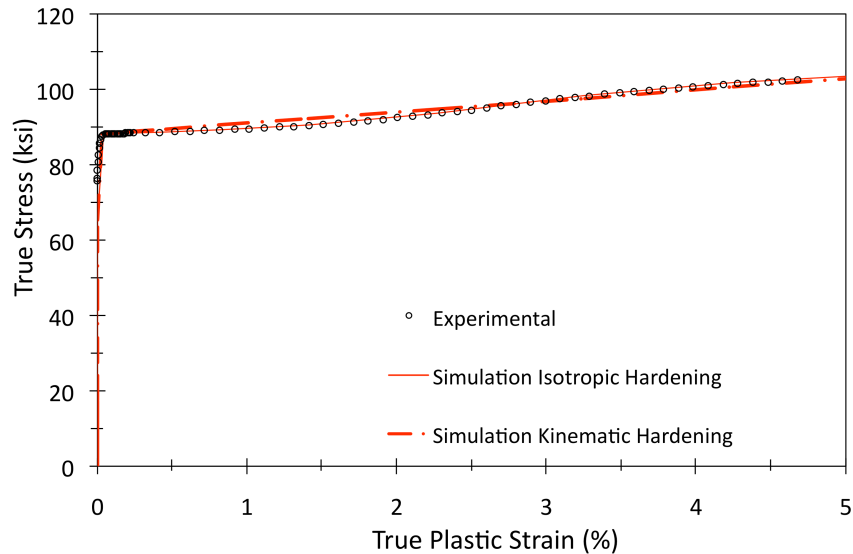


Figure 9. Simulated monotonic response of HY 80 steel.

Figure 10 and Figure 11 depict the correlation between the recorded and predicted relative displacement, and strain time histories for the vertical cantilever specimen CL-3. The relative displacement time history was recorded at the tip of the specimens, where as the strain time history was recorded close to the cantilever base support. In all figures the calculated Russell error factor (Russell, 1997) is also shown for reference. The Russell error factor is an unbiased error measure used for comparing transient signals. Separate error measures are calculated for both magnitude and phase error. These are then combined in a single comprehensive error measure, which accounts for both sources of error. In general, a comprehensive error of less than 0.15 is considered excellent correlation.

A comparison of the time histories presented in Figure 10 and Figure 11 shows that both the isotropic and the kinematic hardening models overestimate the peak relative displacement of the mass and the peak strain at the base of the specimen. While it can be argued that the overestimation of the peak relative displacement and strain values are acceptable, further inspection of Figure 10 and Figure 11 indicates that both the simulations with the isotropic and kinematic hardening models cannot capture the phase of the response after the first peak. For all the results, the Russell comprehensive error factors calculated is above 0.15. While for both models the error factor calculated for the strain correlation is relatively high (0.27), with the

isotropic hardening model, the error factor calculated for the relative displacement of the mass is slightly lower than the one calculated with the kinematic hardening model.

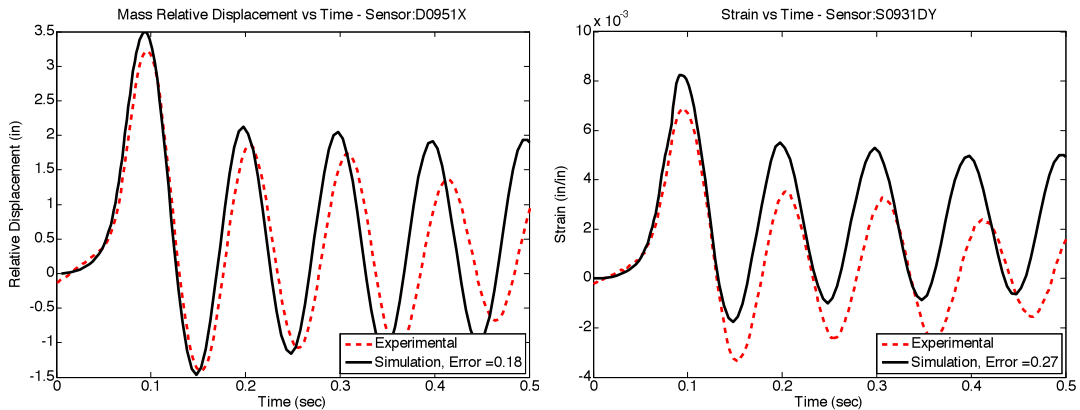


Figure 10. Isotropic hardening: Recorded versus simulated mass relative displacement time history, and strain time history at the base.

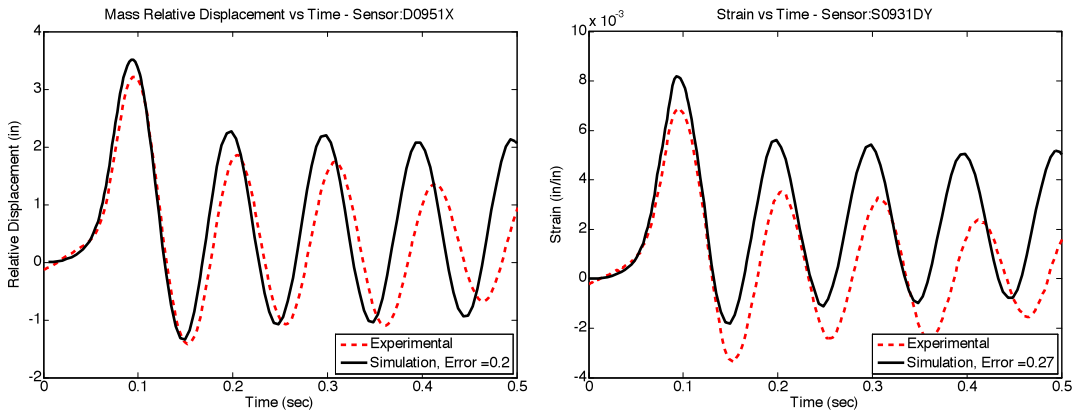


Figure 11. Kinematic hardening: Recorded versus simulated mass relative displacement time history, and strain time history at the base.

When evaluating the result presented in Figure 10 and Figure 11, it is important to note that the strain values the specimen experienced close to its base is well above the yield strain, and the response is highly inelastic. As demonstrated in Figure 9, while with both the isotropic and kinematic hardening models the monotonic stress-strain response of the base material (HY 80) can be accurately simulated, this does not guarantee that the models under consideration can capture

the material response under reversed loading. Figure 12 compares the simulated cyclic response of HY 80 steel with the experimental one for a cyclic loading amplitude of $\Delta\varepsilon/2=0.5\%$.

An inspection of Figure 12 shows the isotropic and the kinematic hardening models, which successfully simulate the monotonic stress-strain response of the base material (Figure 9), cannot capture the shape of the stress-strain loops upon first unloading-reloading. In the problem under consideration, the base material exercised both the initial monotonic plateau response, and the short term hardening on the first load reversal. Since, the unloading-reloading response of the base material is not well presented by the “built-in” plasticity models tested, the global response of the cantilever beam couldn’t be captured accurately.

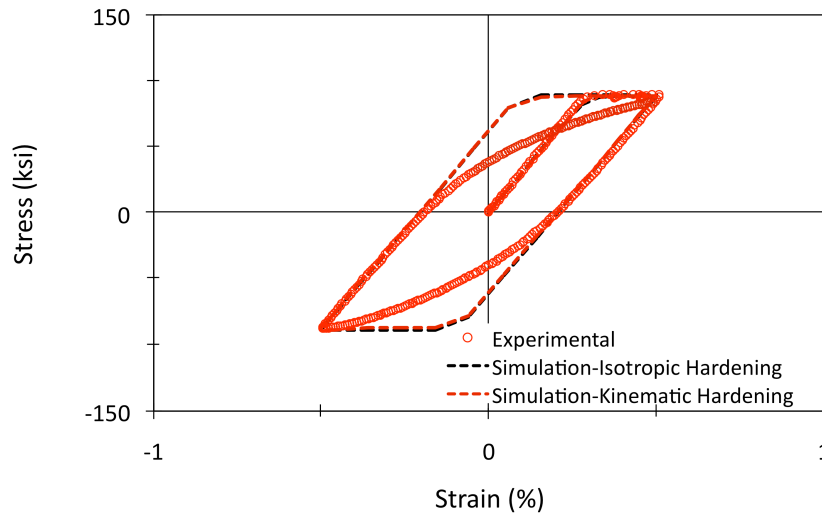


Figure 12. Simulated cyclic response of HY 80 steel.

5. Conclusion

In this paper, the different “built-in” material models for metals available in Abaqus/Standard are evaluated for carbon steels. Through a number of case studies the performance of the different “built-in” models is compared for different load paths. It is shown that two different ‘built-in’ material models which produce the same monotonic stress-strain response, might produce different strain-stress loops under cyclic loading. As a result, validating a material model for a particular load path, does not guarantee that it will produce acceptable results for all the load paths. The analyses results presented herein show the importance of capturing the cyclic stress-strain curve correctly, and that care must be taken in calibration/validation of the material model and the finite element model. Finally, the importance of capturing the shape of the stress-strain loops under cyclic loading is discussed. Although this study deals with carbon steels, the observations reported herein might also be applicable to other metals such as stainless steel.

6. References

1. Hodge, S. C., Minicucci, J. M, and Trimble, T. F., “Cyclic Material Properties Test to Determine Hardening/Softening Characteristics of HY-80 Steel,” General Dynamics Electric Boat, Report No TDA-19195, Groton, CT, 2003.
2. Nakamura, S., Yasunami, H., Kobayashi, Y., Nakagawa, T., and Mizutani, S., “An Experimental Study on the Seismic Performance of Steel Bridge Piers with Less-Stiffened and Compact Sized Section,” Proceedings of the Symposium on Nonlinear Numerical Analysis and Seismic Design of Bridge Piers (JSCE), 1997.
3. Russell, D. M., “Error Measures for Comparing Transient Data; Part I: Development of a Comprehensive Error Measure; Part II: Error Measures Case Study,” Proceedings of the 68th Shock and Vibration Symposium, Hunt Valley, MD, 1997.
4. Trimble, T. F., and Krech, G. R., “Simple Structures Test for Elastic-Plastic Strain Acceptance Criterion Validation,” KAPL Laboratory, Report No KAPL-P-000206, Schenectady, NY, 1997.
5. Ucak, A., and Tsopelas, P., “Realistic Modeling of Structural Steels with Yield Plateau Using Abaqus/Standard,” Proceedings of the 2008 Abaqus Users’ Conference, Newport, RI, 2008.
6. Ucak, A., and Tsopelas, P., “Constitutive Model for Cyclic Response of Structural Steels with Yield Plateau,” Journal of Structural Engineering, ASCE, vol. 137, no. 2, 2011.
7. Ucak, A., and Tsopelas, P., “Accurate Modeling of the Cyclic Response of Structural Components Constructed of Steel with Yield Plateau,” Engineering Structures, Elsevier, vol. 35, page 272-280, 2012.